Ore Geology Reviews 155 (2023) 105375

Contents lists available at ScienceDirect

Ore Geology Reviews

journal homepage: www.elsevier.com/locate/oregeorev

Short communication

Geochronologically constrained life cycles of telescoped porphyry-epithermal systems at the La Arena district, Northern Peru

Alan Santos [a,b], Weimin Guo [c,*], Nian Chen [d], Luis Cerpa [e], Shoji Kojima [f]

[a] Faculty of Earth Resources, China University of Geosciences, Wuhan 430074, China
[b] Andean Zircon Evolution, Mz I 1, Lt5, Pasaje Magnesio, San Juan de Lurigancho, Lima, Peru
[c] Nanjing Center, China Geological Survey, 534 East-Zhongshan Road, China
[d] Ministry of Natural Resources (MNR) Key Laboratory for Exploration Theory and Technology of Critical Mineral Resources, China University of Geosciences, Beijing 100083, China
[e] Peru Geological Survey, Av. Candá 1470, San Borja, Lima, Peru
[f] Universidad Católica del Norte, Av. Angamos 0610, Antofagasta, Chile

ARTICLE INFO

Keywords:
Cooling
Exhumation
Tectonic uplift
Erosion
System preservation
Burial
Apatite (U-Th)/He

ABSTRACT

La Arena and Alizar are porphyry-type Cu-Au-(Mo) deposits with associated Calaorco and Vanessa high-sulfidation epithermal mineralizations, respectively. In this study, we conducted multiple conventional geochronologic analyses on samples from La Arena district, with the objective to obtain precise a temporal relationship among porphyry emplacement, hydrothermal alterations, cooling, exhumation history and preservation, together with published age data for the district.

A precursor quartz–diorite pluton and a late–mineral andesite porphyry bracketed the mineralization in the La Arena and Alizar porphyry deposits. Zircon U-Pb dating of these intrusive rocks display markedly concordant ages, with emplacement beginning and ending at 26.50 ± 0.23 to 25.36 ± 0.07 Ma at La Arena, and at 26.47 ± 0.08 to 25.30 ± 0.07 Ma at Alizar. $^{40}Ar/^{39}Ar$ chronologic data for hydrothermal biotite from the potassic zone ranges from 25.97 ± 0.16 to 25.73 ± 0.16 Ma in the Alizar, and hypogene alunite from the advanced argillic alteration yield an age of 25.66 ± 0.15 Ma in the Vanessa. The weighted mean apatite (U–Th)/He ages of the porphyry intrusions of the La Arena and Alizar range from 24.26 ± 0.56 to 23.42 ± 0.37 Ma.

These geochronologic data reveal that the porphyry systems were emplaced intermittently for at least 1.2 m.y. during the late Oligocene (26.5 – 25.3 Ma). The porphyry intrusions would have been uplifted from its depth of formation at ~ 2 km suggested by telescoped and a short time period (0.07 m.y.; $^{40}Ar/^{39}Ar$ ages) between porphyries and associated high-sulfidation epithermal events. The cooling history from zircon crystallization at 800 °C to thermal collapse at 75 °C (apatite helium close temperature) lasted ~ 2.5 m.y. in the ore-systems. The thermal collapse occurred coeval with the Inca IV orogeny (~24 Ma), period of rapid uplift and exhumation in northern Peru (0.24 km/m.y.; (U-Th)/He age-elevation spectrum). If exhumation continued at the rate of 0.24 km/m.y. unroof of the ore-deposits lasted 5 m.y. (24–19 Ma). Since their exposure at ~ 19 Ma, these ore deposits were subjected to weathering and oxidation during 2.12 m.y. It is thus estimated that approximately 500-m thickness of materials have been removed from the Alizar and La Arena during uplift and erosion, including a large volume of ore. Subsequent volcanic activity occurred during the Quechua I orogeny (~17 Ma) at *ca.* 16.88 Ma, leading to burial and partially preservation of these ore deposits.

1. Introduction

Peru is currently the second largest copper producer in the world with annual production of 2.2 million metric tons (Mt), representing near 10.5% of the world's total copper production (USGS, 2022), mainly derived from Paleocene-early Eocene, middle Eocene-early Oligocene and Miocene-early Pliocene porphyry copper belts (Fig. 1A). The Miocene-early Pliocene metallogenetic belt in central and northern Peru contains porphyry deposits with variable Cu-Au-Ag-Mo-W grades. Porphyry copper–gold systems are emplaced at relatively shallow

* Corresponding author.
E-mail address: mwguo@163.com (W. Guo).

https://doi.org/10.1016/j.oregeorev.2023.105375
Received 6 August 2022; Received in revised form 25 February 2023; Accepted 28 February 2023
Available online 5 March 2023

paleodepths of ~ 2 km (cf. Murakami et al., 2010; Yanites and Kesler, 2015) in convergent plate margins (Sillitoe, 1972; Richards, 2011).

The metals are typically concentrated in confined ore shells (Weis et al., 2012), product of a complex thermal history with fluid flow paths attributed to separate pulsed of magmatic-hydrothermal activity (Dilles and Einaudi, 1992) within of short lifespans (cf. von Quadt et al., 2011; Braxton et al., 2012; Chiaradia et al., 2013). The shallow advanced argillic alteration of the high-sulfidation epithermal environment (Hedenquist et al., 1998; Muntean and Einaudi, 2001; Heinrich et al., 2004) is spatially (Sillitoe, 1973, 2000, 2010; Gustafson and Hunt, 1975; Dilles and Einaudi, 1992), temporally (Arribas et al., 1995; Harrison et al., 2018), and genetically related with porphyry deposits (Hedenquist et al., 1998; Muntean and Einaudi, 2001; Heinrich et al., 2004). The overprint of high-sulfidation mineralization on porphyry deposits is associated with rapid magma cooling and related tectonic uplift with a synmagmatic-hydrothermal activity and the consequent unroof after formation, as a result of either faster erosion under pluvial conditions (Sillitoe, 1994; Masterman et al., 2005; Maydagán et al., 2020) or cooling climate (Sillitoe, 2010; Herman et al., 2013). In northern Peru, late Oligocene telescoped porphyry-epithermal deposits after weathering and oxidation have been partially preserved during continuous cycles of tectonic uplift and erosion (Mégard, 1984; Benavides-Cáceres, 1999; Noble and McKee, 1999) of the volcanic sequences, such as Lagunas Norte (García, 2009; Montgomery, 2012) and La Arena districts (Gauthier et al., 1999; Santos, 2020). Nevertheless, the precise temporal relationship between porphyry emplacement, cooling, burial and regional tectonic uplift have not yet been well elucidated.

As a further investigation to examine the thermal life cycles of the telescoped porphyry-epithermal ore systems at the La Arena district, we focused on direct dating the lifespan from emplacement and hydrothermal alteration, through the cooling and exhumation history, up to exposed at the paleosurface and burial into regional tectonic processes. These multiple geochronological studies constrain the long-live porphyry copper–gold formation at La Arena and Alizar, and the timing and rate of exhumation, as well as the temporal relation to the epithermal-style alteration in conjunction with previous geochronological data on the lifespan of the La Arena porphyry system.

2. Geological setting

The La Arena mineral district is located in the Andes Cordillera of northern Peru (7°53′31.15′′ Lat. S and 78°07′59.44′′ Long. W), approximately 18 km southwest of the Humachuco town and 13 km ENE of the Lagunas Norte mine in northern Peru. The district is a part of the metallogenic province of Oligocene-Miocene age (Noble and McKee, 1999) and contains porphyry copper–gold, and high – sulfidation epithermal deposits, which are hosted by Chicama Triassic shale and siltstone, and Chimú-Farrat Cretaceous quartz-sandstone sediments (Gauthier et al., 1999). These bedded units underwent thin-skinned tectonic movement affected to SW-directional compression during the late Cretaceous to Eocene (Mégard, 1984; Benavides-Cáceres, 1999; Eude et al., 2015; Scherrenberg et al., 2016). A late Middle Eocene (43 –

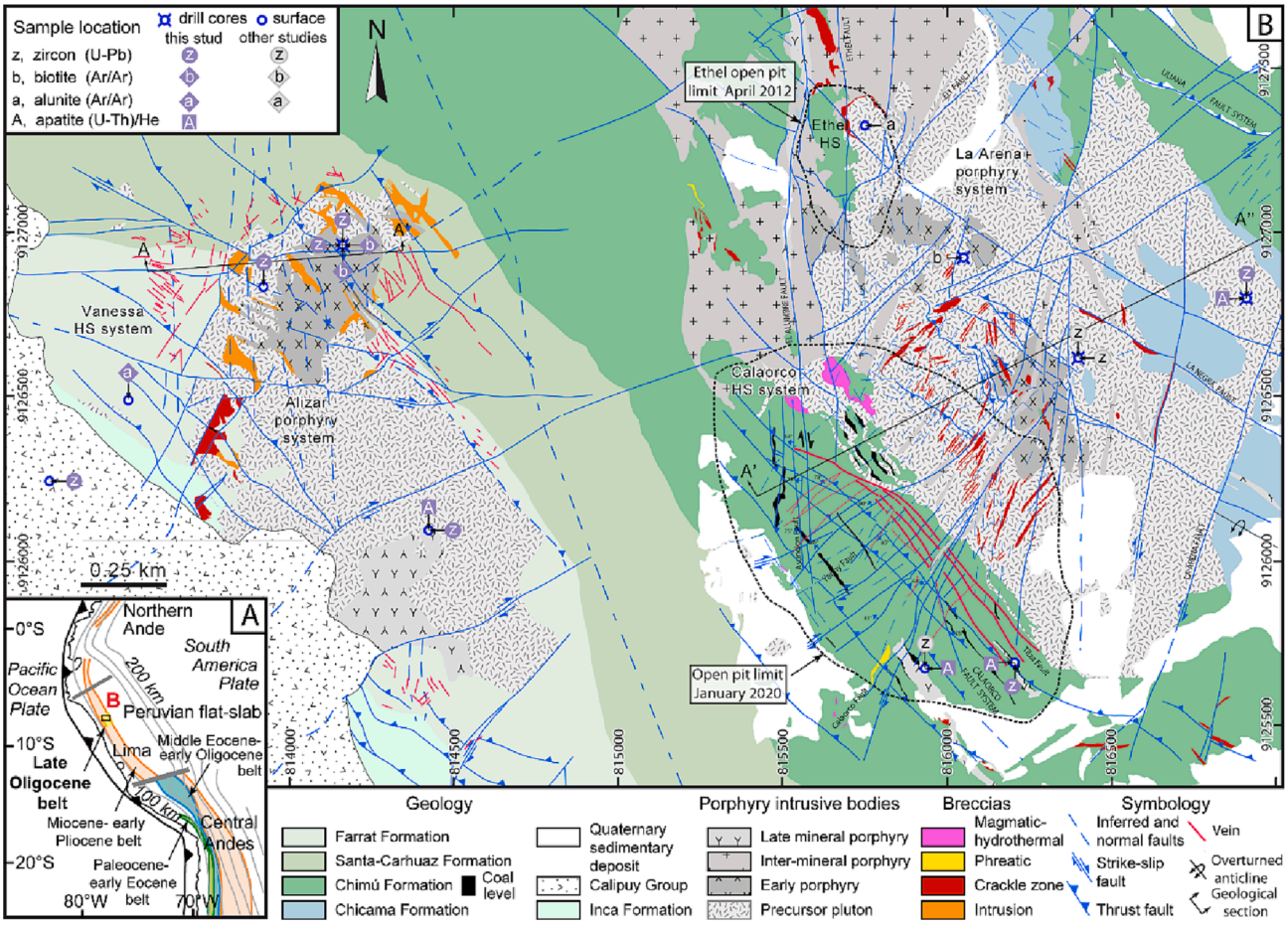

Fig. 1. A. Map showing the location of the Late Oligocene porphyry-epithermal belt relative to other copper belts of the Andes. Modified from Sillitoe and Perelló (2005). The position of the belt within Peruvian flat – slab (amagmatic flat-slab) and South American Pacific margin (modified after Ramos and Folguera, 2009). B. Simplified geologic map of the La Arena and Alizar porphyry systems, based on surface and pit mapping. Modified from Santos (2020). The location of samples collected for zircon U-Pb, biotite-alunite $^{40}Ar/^{39}Ar$, and apatite (U- Th)/He dating are shown as letter (z for zircon, b for biotite, a for alunite, and A for apatite,) referring to the mineral type. Position of the geologic section in Fig. 2 is also shown.

42 Ma) fold and thrust belt developed in the Andes (Benavides-Cáceres, 1999) with the Inca II orogeny, and Huamachuco was a deflection zone between the Andean- and Chimuandes-trend structures (Steinmann, 1929; Hollister, 1977). The Andean structures rotated from NNW to near E-trending (Mégard, 1984), forming the Cajamarca curvature, and record N-S compression (Benavides-Cáceres, 1999; Rousse et al., 2003). The Triassic-Cretaceous sediment rocks were intruded by magmatic phases of the Calipuy Group (Mégard, 1984; Benavides-Cáceres, 1999; Scherrenberg et al., 2016) during the lower Oligocene-to-Middle Miocene (Davies, 2002; Longo et al., 2010; Montgomery, 2012). The first magmatic events were coeval with the Inca III orogeny (Benavides-Cáceres, 1999), that caused the emplacement of the small Milagros dacite porphyry (29.54 ± 0.84 Ma; Montgomery, 2012) at Lagunas Norte and gabbroic dykes (29.4 ± 1.4 Ma; Davies, 2002) along subvertical faults in the Cajamarca districts. This orogeny corresponds to a period of regional upper crustal relaxation and/or extension (Sébrier and Soler, 1991; Davies, 2002). The intense crustal deformation caused by increased convergence rate of ≥ 110 ± 8 km/m.y. at the end of Inca III orogenic phase (Pardo-Casas and Molnar, 1987; Somoza, 1998), coincident with break-up of Farallón Plate into the Cocos and Nazca Plates at ca. 26 Ma (Lonsdale, 2005). The tectonic event was coincident with the first magmatic-hydrothermal activity recorded in the La Arena (Santos, 2020) and subsequently development of the Pampa la Julia erosional surface (Montgomery, 2012).

Miocene magmatism in northern Peru commenced with the Inca IV orogeny (ca. 24 Ma; Noble et al., 1990; Longo, 2005), simultaneous with magmatic-hydrothermal activities at the Michiquillay porphyry Cu–Au–(Mo) (21.9 – 18.7; Marinov, 2011), and El Toro (19.34 – 18.1 Ma; Noble and McKee, 1999; Montgomery, 2012), La Virgen (16.94 ± 0.34 Ma; Noble et al., 2004), and Lagunas Norte (17.4 – 16.5 Ma; Montgomery, 2012; Cerpa et al., 2013) high-sulfidation deposits. Lagunas Norte was associated with an extensive volcanism of the Sauco volcano complex, which mantled the degradational Julia erosional surface recorded close to the base of Calipuy Group in the western margin of the Lagunas Norte district (Montgomery, 2012; Bissig et al., 2015). In northern Peru, Quechua I orogeny corresponds to a major compressive pulse of the Inca fold and thrust belt (~17 Ma; Benavides-Cáceres, 1999; Mégard et al., 1985). It was followed by an erosive period forming the Puna erosional surface (McLaughlin, 1924), generated about 17 m.y. ago (Benavides-Cáceres, 1999) and with La Arena and Lagunas Norte supergene processes at ca. 14 Ma (Montgomery, 2012). These events may have occurred in response to the onset of the Nazca Ridge subduction at ~ 15–11 Ma (Hampel, 2002; Rosenbaum et al., 2005), and with exhumation rate of 0.17–0.27 km/m.y. (Prudhomme et al., 2019).

Geology of the La Arena and Alizar porphyry Cu-Au deposits.

The La Arena and Alizar porphyry deposits are spatially distinct, separated by approximately 2 km of Mesozoic sedimentary sequences of the Chimú and Santa–Carhuaz Formations. These deposits formed in association with two composites. NW – oriented quartz – diorite contain at least three intrusive phases. The intrusions were mostly emplaced into Mesozoic sedimentary rocks (Fig. 1B), and were focused by the preexisting, regional–scale overthrust anticline folded axis of axial trace NW – orientation and SW – vergent. A high–sulfidation mineralization zone is found on the porphyry's southwest shoulders (Fig. 2).

The precursor quartz-diorite intrusion occupies an important volume in the east part of the Calaorco pit and southeast part of the Vanessa. This intrusion has everywhere lower grade of Cu, compared to early andesite porphyry. Significant Cu, Au, and lesser Mo introduction followed this early magmatism, and occurred in association with early and inter-mineral andesite porphyry intrusions at La Arena and Alizar (Fig. 3A, B).

Progressive hydrothermal alteration and veinlet-forming mineralizations affected each of the early and inter – mineral porphyry intrusions, but have different hydrothermal alteration intensity and metal contents in a reflection of multiple magmatic-hydrothermal cycles (Santos, 2020). The hydrothermal alteration of the La Arena and Alizar porphyry deposits conforms to the gold-rich porphyry zonal pattern, in which early potassic core is widely overprinted by sericite-chlorite (SCC) alteration zone. Both zones are laterally bordered by an annular sericitic zone. The sericite-chlorite zone is surrounded by a propylitic halo in deeper areas, and the shallow area is superimposed by an extensive advance argillic alteration. The bulk of the hypogene metal resource is hosted by the sericitic and sericite–chlorite zones as veinlets and disseminated.

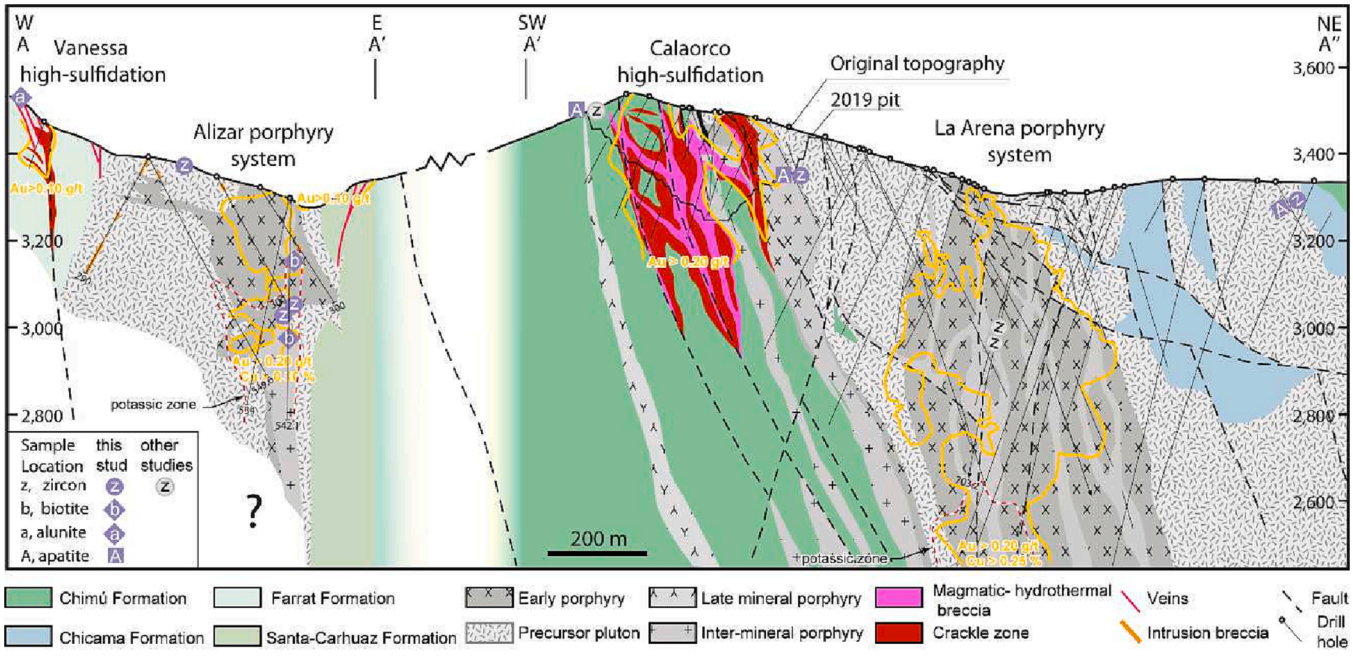

Fig. 2. A southwest-northeast transverse geological section (looking NW). At La Arena, spatial relationship between porphyry and epithermal ore systems, vertically extensive of deeper potassic hydrothermal alteration zone and copper–gold grades distribution, compared with Alizar largely eroded system. Relationships are based on interpretation and assay from drill cores (gray lines). Modified from Santos (2020). Cross section also shows the vertical location of the collected samples and position of cross section given in Fig. 1B.

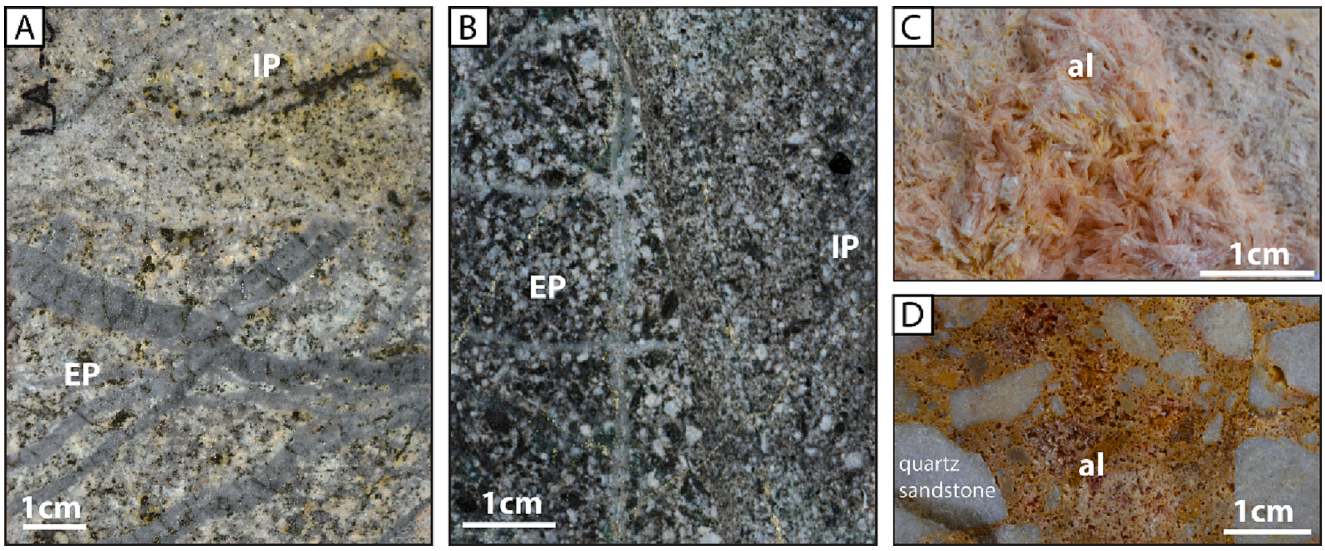

Fig. 3. Early andesite porphyry (EP) with early wavy A-type quartz veinlets, and overprinted pervasive altered and mineralized by sericite (A), and hydrothermal biotite – magnetite (B) + quartz with disseminated pyrite, chalcopyrite and gold. After this first pulse of magmatic-hydrothermal mineralization, A – quartz veinlets are truncated along a subvertical contact with an inter – mineral andesite porphyry (IP), and then both magmatic-hydrothermal pulses are cut by pyrite-bearing veinlets. C) Alunite present in the advanced argillic alteration assemblage in as early andesite Ethel high-sulfidation area. D) Alunite filling in oxidized hydrothermal breccia matrix of the Vanessa advanced argillic-altered lithocap.

The Calaorco and Vanessa lithocaps are superimposed on the porphyry's southwest shoulder, as an offset from the causative porphyry suites (Fig. 2). These ore-deposits are partially covered by Calipuy Group volcanic rocks. The lithocaps are composed predominantly of hematitic-goethitic leached capping that attains up to 400 m thick at Calaorco, whereas a locally restricted and deeply eroded lithocap at Vanessa (Santos, 2020). The hydrothermal alteration is zoned outward and downward, with decreasing SiO_2 and Au contents through quartz – pyrophyllite – alunite ± diaspore to quartz – dickite – kaolinite ± alunite. The oxidized high-sulfidation gold mineralization is hosted in hydrothermally non – reactive Chimú quartz – sandstone, bedding planes, multiple stages of brecciation and silicification controlled by a series of northwest- and northeast-trending faults systems (Figs. 1, 2). In the hematitic-goethitic capping, lenses of mixed zones with hypogene mineralization are relatively uncommon, and consist mainly of pyrite, enargite, luzonite, covellite and Au.

The La Arena porphyry resource contains 742.4 Mt @ 0.35% Cu and 0.24 g/t Au, for 2.626 Mt Cu and 159.81 t Au. There is additional 2.450 Moz Au in Calaorco oxidized high-sulfidation epithermal mineralization (J. Perez, pers. commun., 2022). The oxidized gold has largely been mined out by Pan American Silver.

Previous geochronological data of magmatism and hydrothermal activity at the La Arena-Calaorco porphyry epithermal deposits (Santos, 2020) demonstrate that the magmatic-hydrothermal pulses from precursor quartz – diorite pluton to late – mineral andesite porphyry were developed in a timespan<2.24 m.y., from 26.64 to 24.40 Ma. Moreover, published data of $^{40}Ar/^{39}Ar$ age (Montgomery, 2012; Santos, 2020) from alunites and hydrothermal biotites define two magmatic-hydrothermal pulses at La Arena that spanned ~ 0.89 m.y. from 26.40 to 25.51 Ma. The first pulse of magmatic– hydrothermal activity is observed at northwest part of the La Arena and occurred at 25.81 Ma in the Ethel area (Fig. 1); afterwards the magmatic – hydrothermal activity migrated to southwest. The second magmatic–hydrothermal activity became widespread by 25.51 Ma in the Calaorco. The deeper porphyry – style hydrothermal biotite from SCC alteration zone at La Arena (25.96 Ma) is synchronous with the hypogene alunite from Ethel area (25.81 Ma) and ~ 0.39 m.y. older than the alunites from Calaorco, suggesting that the preserved advanced argillic alteration over the top of the porphyry was formed during the second magmatic – hydrothermal pulse.

A poorly defined plateau supergene alunite age of ~ 14 Ma was obtained (Montgomery, 2012), suggesting that the oxidation at Calaorco may have occurred in the Early Miocene.

3. Samples and geochronological methods

A suite of samples was collected from the La Arena and Alizar porphyry systems to carry out zircon U-Pb and biotite – alunite $^{40}Ar/^{39}Ar$ and apatite (U-Th)/He chronometric analyses. These ages coupled with previously reported geochronological ages (Santos, 2020) to establish the lifespans of magmatism, hydrothermal activity, and exhumation of these porphyry systems.

Fieldwork focused on collecting seven samples with unambiguous field relationships (Fig. 3), including two precursor quartz-diorite intrusions and two late-mineral andesite porphyries from the Calaorco-La Arena and Alizar deposits, which pre and postdate essentially all Cu – Au ± Mo mineralization. Two andesite porphyries related with metal introduction were obtained from drill core in the Alizar porphyry system. To constrain the timing of burial of the exhumed Alizar porphyry system, a sample of block-ash flow volcanic sequence, were collected at the lower stratigraphic level of the Calipuy Group (near the basal unconformity), which covers a main the southwest extension of the Alizar porphyry system profile (Fig. 1B). Separated zircon grains from rock samples were characterized texturally by cathodoluminescence, reflected- and transmitted-light images. Selected zircon crystals have typical magmatic origin with oscillatory-zoned bands and without inclusions were subsequently analyzed by a laser ablation inductively couple plasma spectrometer (LA – ICP – MS) housed at the Institute of Geochemistry, Chinese Academy of Sciences, Guiyang. The obtained age results were employed to constrain the absolute timing and duration of magmatism.

Two drill core porphyry-style biotite alteration samples with Cu – Fe sulfides at the Alizar porphyry deposit and a shallower coarse alunite in quartz – alunite – altered matrix in monolithologic magmatic-hydrothermal breccia at the Vanessa lithocap (Fig. 1B) were collected and analyzed using a thermos multi-collector ARGUS VI noble gas mass spectrometer housed at the Key Laboratory of Tectonics and Petroleum Resources, Ministry of Education, China University of Geosciences, Wuhan.

Apatite grains were separated from four samples, which collected from drill core and surface area over a vertical interval of 212 m of La

Arena – Alizar intrusive complex (Fig. 1B). The inclusion – free euhedral apatite grains with size>100 μm long and 70 μm wide were selected and analyzed.

The apatite analyses were performed by an alphachron and ICP-MS housed at the Institute of Geochemistry, Chinese Academy of Sciences, Guiyang.

Detailed analytical methods, sample locations, analytical data, Concordia plots, and spectra and isochrones for all analyzed samples are reported in the Tables S1 to S6 and Figs. S1 and S2 (Supplementary Materials).

3.1. Zircon U-Pb, biotite – alunite $^{40}Ar/^{39}Ar$, and apatite (U-Th)/He dates

U-Pb LA – ICP – MS dating of igneous zircons samples of the precursor quartz – diorite yielded an age of 26.50 ± 0.23 Ma (MSWD = 0.91, n = 17) from the La Arena and 26.47 ± 0.08 Ma (MSWD = 0.73, n = 20) from the Alizar porphyry deposit. LA – ICP – MS dating of the early – and inter – mineral porphyry from the Alizar gave ages of 26.33 ± 0.32 (MSWD = 0.53, n = 17) and 25.90 ± 0.28 Ma (MSWD = 1.05, n = 15), respectively. Similar dating of the late-mineral porphyries yielded ages of 25.36 ± 0.07 (MSWD = 0.78, n = 24), and 25.30 ± 0.07 Ma (MSWD

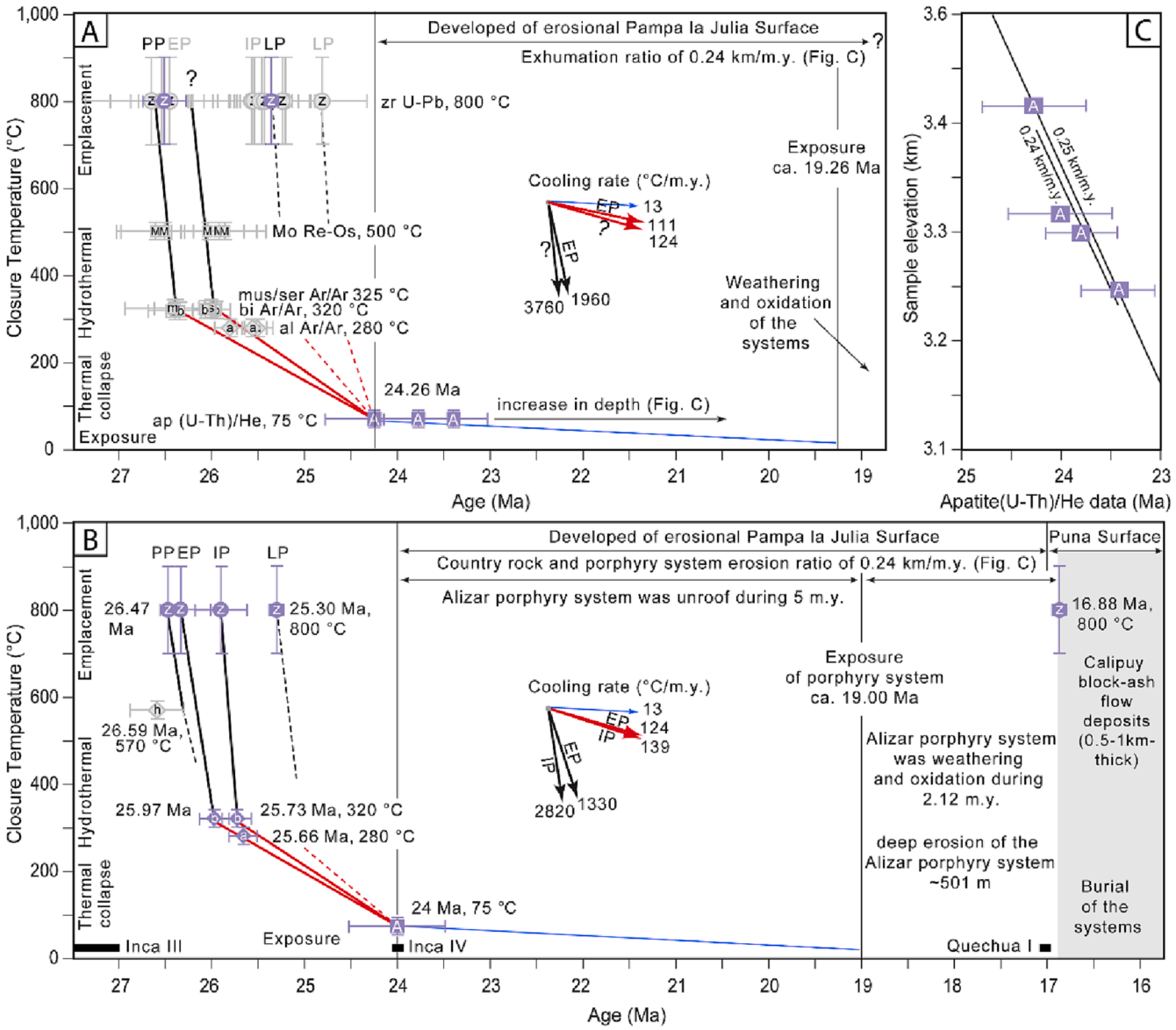

Fig. 4. Summary diagram of integrated zircon U-Pb, biotite-alunite $^{40}Ar/^{39}Ar$, and apatite (U- Th)/He data from La Arena and Alizar, are also plotted here U-Pb, Re-Os, and $^{40}Ar/^{39}Ar$ data (gray symbols) reported by Montgomery (2012) and Santos (2020), which records a complete cooling history of the La Arena-Calaorco (A) and Alizar-Vanessa (B) porphyry-epithermal systems. All age determinations are shown with 2σ uncertainty. Results of geochronological data reveal multiple cooling path with rapid to moderate cooling rates (°C/m.y.) as a result of each of the porphyry intrusions (PP: precursor pluton, EP: early porphyry, IP: inter-mineral porphyry, and LP: late-mineral porphyry). The protracted cooling history at La Arena and Alizar lasted ~ 7.46 and ~ 7.12 m.y., from emplacement and associated hydrothermal activity in 0.25 and 0.36 m.y. (black lines, dashed where uncertain), through thermal collapse in 2.21 and 1.76 m.y. (red lines, dashed where uncertain), to common exposure interval of 5 m.y. (blue lines), respectively. Weathering and oxidized during 2.12 m.y. led to deep erosion (~500 m thick) at Alizar, comparable with preserved leach capping (~400 m thick) at adjacent La Arena. Subsequent volcanic activity at ca. 16.88 ± 0.05 Ma, leading to burial of the deposits and partially preservation of the telescoped porphyry-epithermal systems. C. Age-elevation diagram for apatite (U-Th)/He dating results (2σ) from La Arena and Alizar. Data ages plot on a well-defined younging trend with increasing depth, error-weighted slope of 0.24 and 0.25 km/m.y., consistent with 0.24 km of rapid exhumation at ~ 24 Ma best fits existing data. (For interpretation of the references to colour in this figure legend, the reader is referred to the web version of this article.)

= 0.68, n = 21) from the La Arena and Alizar porphyry deposits, respectively. A Calipuy block-ash flow sample gave an age of 16.88 ± 0.05 Ma (MSWD = 0.78, n = 19) (Fig. 4; Table S1).

$^{40}Ar/^{39}Ar$ determination of deeper porphyry-style hydrothermal biotite related with early and inter – mineral andesite porphyries from Alizar yielded undisturbed plateau ages of 25.97 ± 0.16 and 25.73 ± 0.16 Ma, respectively. Hypogene bladed-coarse alunite from the Vanessa lithocap yielded a relatively younger plateau age of 25.66 ± 0.15 Ma (Fig. 4; Table S2).

The apatite samples from La Arena-Alizar apatite display (U-Th)/He ages ranging from 24.26 ± 0.52 to 23.42 ± 0.37 Ma for the same sample used for zircon U-Pb dating. The thermochronology to dating the low-temperature cooling and exhumation history for the precursor quartz – diorite from the La Arena porphyry deposit yielded single grain (U–Th)/He ages between 30.23 and 18.75 Ma, with mean (U–Th)/He age of 23.42 ± 0.37 Ma (n = 7). The scattered of the U–Th/He ages of the quartz-diorite suggests, at a first glance, that this rock was subjected to a moderate-strong propylitic alteration. The late – mineral andesite dike from the bottom of the Calarco open pit yielded single grain (U–Th)/He ages between 25.80 and 21.22 Ma, with a mean (U–Th)/He age of 23.79 ± 0.36 Ma (n = 9). Late-mineral porphyry intrusion from the top of the Cerro Calaorco gave (U–Th)/He ages between 25.65 and 22.62 Ma, with a mean (U–Th)/He age of 24.26 ± 0.52 Ma (n = 4). Finally, late-mineral andesite from the Alizar porphyry system yielded (U–Th)/He ages between 29.14 and 22.20 Ma, with a mean (U–Th)/He ages of 24.00 ± 0.52 Ma (n = 4). All four mean apatite (U–Th)/He ages are significantly younger than the zircon crystallization ages of the sampled porphyries (Fig. 4; Table S3), and show a positive correlation with elevation into the intrusive complexes, as expected decrease in ages for exhumation-induced cooling through apatite helium closure–temperature.

4. Discussion

4.1. Spatial and temporal relationship of porphyry-style and epithermal alteration at Alizar and La Arena

The magmatic-hydrothermal advanced argillic alteration associated with the Calaorco-Ethel and Vanessa high-sulfidation gold mineralization zones are laterally offset up to ~ 0.6 and ~ 0.4 km from the surface projection of the causative La Arena and Alizar porphyry-style alteration zones, respectively (Fig. 1B, 2). Similar magmatic-hydrothermal relations are reported in Far Southeast-Lepanto, Philippines (Hedenquist et al., 1998) and Yanacocha, Peru (Longo et al., 2010). The $^{40}Ar/^{39}Ar$ dates indicate that deep porphyry-style hydrothermal biotite from the Alizar early porphyry (25.97 ± 0.16 Ma) is ~ 0.31 m.y. older than the overlying Vanessa advanced argillic alteration (25.66 ± 0.15 Ma). However, advance argillic alteration and porphyry – style alteration and Cu – Au mineralization are documented to have occurred in a very short time-period on telescoped porphyry-epithermal systems (0.08 m.y.; Harrison et al., 2018). Else, the hydrothermal biotite $^{40}Ar/^{39}Ar$ age from the Alizar inter-mineral porphyry (25.73 ± 0.16 Ma) is statistically similar within a 2σ error (0.07 m.y) to the shallow hypogene Vanessa quartz – alunite alteration lithocap. Similar variations in age range are reported at Calaorco – Ethel – La Arena porphyry and epithermal deposits (Santos, 2020). This implies that the bladed-coarse grained alunite from the Calaorco-Ethel and Vanessa advanced argillic alteration (as district-scale lithocap) may have crystallized directly from a SO_2-rich magmatic vapor fluid-flow path that ascended highly rapidly to prevent reduction of SO_2 to H_2S (cf. Rainbow et al., 2005). This fluid formed contemporaneously the deeper biotite-bearing potassic alteration zone associated with the intermineral andesite porphyry intrusion deep in the La Arena and Alizar deposits.

4.2. Longevity of the La Arena – Alizar porphyry systems

The transport metal-bearing volatiles in the La Arena and Alizar porphyry systems are associated with the early – and inter – mineral porphyry stocks. The intrusion of the main intensely mineralize early andesite porphyry at Alizar commenced immediately after the emplacement of the precursor pluton, i.e., at 26.33 ± 0.32 Ma in time gap of up to ~ 0.14 m.y. at Alizar, and ~ 0.05 m.y. at La Arena porphyry deposit (Santos, 2020). These time gaps are highly consistent with the previous studies, such as Dilles and Wright (1988) and Sillitoe and Mortensen (2010). A weak mineralized inter-mineral porphyry at 25.90 ± 0.90 Ma closely follows the main mineralization centered on the Alizar early porphyry, although with relative chronology field evidences for a magmatic lull of at least 0.43 m.y., and 0.90 m.y. in the La Arena porphyry system (Santos, 2020), characterized by chilled subvertical porphyry contacts (Fig. 3A, B).

The magmatic-hydrothermal alteration and metal introduction at the La Arena and Alizar porphyry deposits are bracketed by a precursor quartz – diorite pluton and late – mineral andesite porphyry intrusions, developed over a similar interval of 1.14 ± 0.24 and 1.17 ± 0.11 m.y., according to the zircon U-Pb ages from 26.50 ± 0.23 to 25.36 ± 0.07 Ma and 26.47 ± 0.08 to 25.30 ± 0.07 Ma, respectively. The lifespan of the La Arena porphyry deposit is previously reported about 2.24 ± 0.79 m.y. (Santos, 2020), where the time interval was calculated based on a younger late – mineral andesite porphyry intrusion (~24.81 Ma). Therefore, the mineralization at the La Arena and Alizar ended at about ~ 25.35 Ma, i.e., about ~ 1.2 m.y. after the main magmatic-hydrothermal activity (26.5 – 25.3 Ma), on the assumption that the younger porphyry intrusion probably reflects magmatic-hydrothermal resurgence in the magma chamber. Thus, the magmatic-hydrothermal systems at La Arena and Alizar have a similar and relatively long life-span. Furthermore, La Arena is the very large size deposit (cf. Clark, 1993) that evolved along complex fluid flow paths as separate pulses of hydrothermal activity associated with multiple intrusions of porphyry plugs through Late Oligocene may account for this significantly long duration (~1.2 Ma). However, the duration estimate of the La Arena – Alizar porphyry deposits can be compared to the lifespan of magmatic-hydrothermal systems at Boyongan and Bayugo, Philippines (0.2 m.y., Braxton et al., 2018), Toromocho, Peru (3.5 m.y. Catchpole et al., 2015), Cerro la Mina, Mexico (0.35 m.y., Jansen et al., 2017), Luoboling – Zijinshan porphyry and epithermal systems, China (2 m.y., Pan et al., 2019), Golpu – Wafi porphyry and epithermal systems, Papua New Guinea (0.1 m.y., Rinne et al., 2018), Cerro de Pasco, Peru (1.2 m.y., Rottier et al., 2018).

4.3. Cooling, exhumation history, and preservation conditions of the telescoped porphyry-epithermal systems

The La Arena – Alizar porphyry intrusions were emplaced during a period of regional compressional and uplift at the end of the Inca orogenic phase (30 – 27 Ma; Benavides-Cáceres, 1999), representing initiation of regional stress relaxation (cf. Tosdal and Richards, 2001). Zircon U-Pb, biotite – alunite $^{40}Ar/^{39}Ar$, and apatite (U–Th)/He data reflect multiple cooling path with rapid to moderate cooling rates as a product of each pulse of magmatic – hydrothermal activity related to porphyry intrusions. The cooling paths are grouped in three episodes during the thermal life cycles from emplacement to exposure of the La Arena – Alizar orebodies, which are summarized in Fig. 4A, B. The La Arena porphyry complex presents a first steep rapid cooling episode of 3760 – 1960 °C/m.y. following the magmatic-hydrothermal activity (26.50 – 25.96 Ma). These ages suggest that the porphyry intrusions and their hydrothermal system cooled below the closure temperatures from zircon U–Pb (>800 °C; Cherniak and Watson, 2000), followed by molybdenite Re-Os (500 °C; Suzuki et al., 1996), to muscovite (325 °C; Snee et al., 1988), and biotite argon (320 ± 20 °C; McDougall and Harrison, 1999) in about 0.25 m.y. or less (cf. Harris et al., 2008). In

contrast, the Alizar porphyry deposit shows a slight decrease in slope of the cooling path with rate of 2820–1330 °C/m.y. from ages U–Pb zircons at 26.47 – 25.30 Ma, and the $^{40}Ar/^{39}Ar$ age data (25.97 – 25.73 Ma) of the potassic biotite suggest a cooled magmatic – hydrothermal system lasting of ~ 0.36 m.y. The rapid cooling of the porphyry system during the early stage may be the result of the fast heat transfer and thermal relaxation between wall-rock and high temperature fluid (Yin et al., 2019) in relatively shallow depth of formation (~2.1 km in average; Murakami et al., 2010). However, the rapid cooling at La Arena and Alizar is also registered during mineralization and hydrothermal alteration stages, suggesting a fast metal – rich fluids release from the underlying parental chamber and its synchronous solidification.

The slope of the second cooling episode at the La Arena decreases considerably at a ratio of 124 – 111 °C/m.y. (Fig. 4A), from their deep porphyry-style hydrothermal biotite alteration zones, through shallow hypogene alunite at 25.81–25.51 Ma (Santos, 2020), to apatite from the late-mineral porphyry in the surface area at 24.26 ± 0.52 Ma. The apatite (U–Th)/He ages records the thermal collapse time when the rocks rise to ~ 2–1 km depth (40 °C isotherm) into the helium partial retention zone (HePRZ; Farley, 2002), where helium is quantitatively retained by apatite. Based on this premise, the $^{40}Ar/^{39}Ar$ and (U–Th)/He ages suggest that this magmatic-hydrothermal system thermally collapsed from biotite and alunite (280 ± 7 °C; Lovera et al., 1997) argon closure temperatures to apatite helium closure temperature (75 ± 7 °C; Wolf et al., 1996) in a span of < 2.21 m.y. The Alizar porphyry system may have a similar second cooling history to the La Arena porphyry deposit with a cooling ratio of 124 – 139 °C/m.y. (Fig. 4B), which suggests that the magmatic – hydrothermal system thermally collapsed in ~ 1.76 m.y. or less. Thus, the cooling history from zircon crystallization at 800 °C to the thermal collapse of the La Arena-Alizar porphyry systems at 75 °C lasted ~ 2.5 m.y., assuming that during this period the porphyry intrusions have been uplifted from its depth emplacement at ~ 5 – 4 km to depths shallower than ~ 2 km, as suggested by field characteristics (overprinted of epithermal on porphyry mineralizations; e.g. Maydagán et al., 2020). These parameters give rise to inferred exhumation rates of 0.8 – 0.4 km/m.y., which are consistent with the previous exhumation and erosion rates reported on several porphyries in the southern Andes, such as the porphyry copper deposits of North Chilean Precordillera (>0.30 km/m.y.; Dahlström et al., 2022), El Teniente, Chile (ca. 0.62 km/m.y.; McInnes et al., 2005), and Altar Region, Argentina (ca. 0.5–1 km/m.y.; Maydagán et al., 2020). However, these ratios are orders of magnitude higher than the general average exhumation rate of 0.158 km/m.y. for the common Phanerozoic porphyry deposits (Kesler and Wilkinson, 2006). The best-defined average exhumation ratio in the La Arena district is determined through projecting from the apatite age-elevation profile in the order of 0.24 km/m.y. (Fig. 4C), comparable with regional exhumation and erosion ratios of 0.17 – 0.27 km/m.y. estimated for the Miocene in the northern Peruvian Andes (Prudhomme et al., 2019).

Considering a mean annual surface temperature of 10 ± 5 °C, constant geothermal gradient of 30 °C/km and the use of conduction rate equation - Fourier's law, this temperature range is equivalent to at most ~ 1.2 km thick sediment-volcanic pile to have covered the porphyry systems.

If exhumation continued at the rate of 0.24 km/m.y., exposure and weathering of the current surface area initiated ca. 19.26 Ma at La Arena and ca. 19.00 Ma at Alizar with a cooling rate of 13 °C/m.y., formed during and after of the uplift and subsequent erosion related to the Inca IV orogenic phase (~24 Ma; Navarro et al., 2010). The burial process of the Alizar began at ca. 16.88 ± 0.05 Ma by a 500 – 1000 m-tick block-ash flow volcanic sequences of the Sauco volcano complex (Montgomery, 2012), not buried sufficiently to reset the (U–Th)/He system. These post-ore volcanic sequences provide a favorable environment to partially controlled the removal of the leached profile of the Alizar porphyry (~500 m depth of erosion) developed during a protracted time surface exposure (~2.12 m.y.) where some root zones of advance argillic alteration were still preserved (Fig. 2).

The La Arena apatite (U–Th)/He ages and the presence of remanent volcanic deposits uncoformably underlie an advanced argillic – alteration quartz sandstone in the northwestern part of the Calaorco pit, suggesting that it may have given an analogous burial process to the Alizar porphyry deposit. However, supergene alunite age and isotopic data on goethite from the Calaorco (Montgomery, 2012), indicate that the oxidation of the surface exposure may have partially continued to ca. 14 Ma or exposed again during the Middle Miocene. This protracted time exposure (~5 m.y.) supports the poor preservation of the La Arena oxidation profile (<50 m). In contrast, the preservation of a vertically extensive oxidized high-sulfidation profile in Calaorco (~400 m) developed on the Arena porphyry shoulder was probably due to high permeability of the quartz sandstone, producing the vertically extensive vadose zone of oxidation.

5. Conclusions

The copper–gold mineralization in the Late Oligocene La Arena porphyry district occurred at a time of relatively fast exhumation ratio, consistent with previous thermochronological studies and regional models in northern Peru. The regional models suggest that high exhumation rates favor hypogene mineral generation by promoting efficient mineralizing fluid exsolution and enable epithermal-mineralization telescoping. The thermal collapse occurred synchronously with the Inca IV orogeny (~24 Ma) with an exhumation ratio of 0.24 km/m.y. becoming exposed at ~ 19 Ma, followed by deeply weathering (~500 m of erosion in the Alizar porphyry) and oxidation (~400 m of leached capping in the Calaoco deposit). The buried of these porphyry deposits occurred with an extensive Miocene Calipuy volcanism attributed to Mid-Miocene controlled by a regional contractional Quechua I orogeny (~17 Ma), which indicates that this orogeny had a significant impact on the preservation of the Oligocene porphyry ore systems towards to west of the La Arena district.

Declaration of Competing Interest

The authors declare that they have no known competing financial interests or personal relationships that could have appeared to influence the work reported in this paper.

Data availability

Data will be made available on request.

Acknowledgments

The geological framework presented was developed a part of Santos's master thesis at the China University of Geosciences, Wuhan. We wish to express our gratitude to the Natural Science Foundation of China (No. 41302071 and No. 2021YFC2901804), Minera Tahoe Resources Inc., and Andean Zircon Evolution for their support in the logistics of obtaining the La Arena district samples and information generated during their exploration stages. We wish to acknowledge the many La Arena mining exploration geologists, particularly Raúl Jiménez, Wilder Garcia, Ricardo Gordillo, Jhuleyssy Sánchez, Saúl Arias, and Isaac Barboza, Julio Perez who guided to the lithocaps generation in quartz sandstone rocks in the La Arena district. We give special thanks to Thomas Bissig and Enrique Garay for their critical reviews and valuable comments to greatly improve the content of the manuscript.

Appendix A. Supplementary data

Supplementary data to this article can be found online at https://doi.org/10.1016/j.oregeorev.2023.105375.

References

Arribas, A., Hedenquist, J.W., Itaya, T., Okada, T., Concepcion, R.A., Garcia, J.S., 1995. Contemporaneous Formation of Adjacent Porphyry and Epithermal Cu-Au Deposits over 300 Ka in Northern Luzon, Philippines. Geology 23, 337–340.

Benavides-Cáceres, V., 1999. Orogenic Evolution of the Peruvian Andes: The Andean Cycle. In: Skinner, B.J. (Ed.), Geology and Ore Deposits of the Central Andes. Society of Economic Geologists, pp. 61-107.

Bissig, T., Clark, A.H., Rainbow, A., Montgomery, A., 2015. Physiographic and tectonic settings of high-sulfidation epithermal gold–silver deposits of the Andes and their controls on mineralizing processes. Ore Geol. Rev. 65, 327–364.

Braxton, D.P., Cooke, D.R., Dunlap, J., Norman, M., Reiners, P., Stein, H., Waters, P., 2012. From crucible to graben in 2.3 Ma: A high-resolution geochronological study of porphyry life cycles, Boyongan-Bayugo copper-gold deposits, Philippines. Geology 40, 471–474.

Braxton, D.P., Cooke, D.R., Ignacio, A.M., Waters, P.J., 2018. Geology of the Boyongan and Bayugo Porphyry Cu-Au Deposits: An Emerging Porphyry District in Northeast Mindanao, Philippines. Econ. Geol. 113, 83–131.

Catchpole, H., Kouzmanov, K., Bendezú, A., Ovtcharova, M., Spikings, R., Stein, H., Fontboté, L., 2015. Timing of porphyry (Cu-Mo) and base metal (Zn-Pb-Ag-Cu) mineralisation in a magmatic-hydrothermal system—Morococha district, Peru. Miner. Deposita 50, 895–922.

Cerpa, L.M., Bissig, T., Kyser, K., McEwan, C., Macassi, A., Rios, H.W., 2013. Lithologic controls on mineralization at the Lagunas Norte high-sulfidation epithermal gold deposit, northern Peru. Miner. Deposita 48, 653–673.

Cherniak, D.J., Watson, E.B., 2000. Pb diffusion in zircon. Chem. Geol. 172, 5–24.

Chiaradia, M., Schaltegger, U., Spikings, R., Wotzlaw, J.-F., Ovtcharova, M., 2013. How accurately can we date the duration of magmatic-hydrothermal events in porphyry systems?—an invited paper. Econ. Geol. 108, 565–584.

Clark, A.H., 1993. Are outsize porphyry copper deposits either anatomically or environmentally distinctive? Soc. Econom. Geol. Special Publication 2, 213–283.

Dahlström, S.I.R., Cooper, F.J., Blundy, J., Tapster, S., Yáñez, J.C., Evenstar, L.A., 2022. Pluton Exhumation in the Precordillera of Northern Chile (17.8°–24.2°S): Implications for the Formation, Enrichment, and Preservation of Porphyry Copper Deposits. Econ. Geol. 117, 1043–1071.

Davies, R.C.I., 2002. Tectonic, magmatic and metallogenic evolution of the Cajamarca mining district, Northern Peru. James Cook University, Queensland, Australia. Ph. D thesis.

Dilles, J.H., Einaudi, M.T., 1992. Wall-rock alteration and hydrothermal flow paths about the Ann-Mason porphyry copper-deposit, Nevada - a 6-Km vertical reconstruction. Econ. Geol. 87, 1963–2001.

Dilles, J.H., Wright, J.E., 1988. The chronology of early Mesozoic arc magmatism in the Yerington district of western Nevada and its regional implications. Geol. Soc. Am. Bull. 100, 644–652.

Eude, A., Roddaz, M., Brichau, S., Brusset, S., Calderon, Y., Baby, P., Soula, J.C., 2015. Controls on timing of exhumation and deformation in the northern Peruvian eastern Andean wedge as inferred from low-temperature thermochronology and balanced cross section. Tectonics 34, 715–730.

Farley, K.A., 2002. (U-Th)/He Dating: Techniques, Calibrations, and Applications. Rev. Mineral. Geochem. 47, 819–844.

García, W.V., 2009. Geology of the Milagros Project, Alto Chicama district, La Libertad. Colorado School of Mines, Colorado, USA. Peru (M.Sc thesis).

Gauthier, A., Díaz, N., Quirita, V., 1999. Yacimientos La Arena-Virgen. [abs.]: Primero Congreso Internacional de Prospectores y Exploradores, Lima 1999, Instituto de Ingeniero de Minas del Perú, pp. 73-91.

Gustafson, L.B., Hunt, J.P., 1975. The porphyry copper deposit at El Salvador, Chile. Econ. Geol. 70, 857–912.

Hampel, A., 2002. The migration history of the Nazca Ridge along the Peruvian active margin: a re-evaluation. Earth Planet. Sci. Lett. 203, 665–679.

Harris, A.C., Dunlap, W.J., Reiners, P.W., Allen, C.M., Cooke, D.R., White, N.C., Campbell, I.H., Golding, S.D., 2008. Multimillion year thermal history of a porphyry copper deposit: application of U-Pb, 40Ar/39Ar and (U–Th)/He chronometers, Bajo de la Alumbrera copper–gold deposit, Argentina. Miner. Deposita 43, 295–314.

Harrison, R.L., Maryono, A., Norris, M.S., Rohrlach, B.D., Cooke, D.R., Thompson, J.M., Creaser, R.A., Thiede, D.S., 2018. Geochronology of the Tumpangpitu Porphyry Au-Cu-Mo and High-Sulfidation Epithermal Au-Ag-Cu Deposit: Evidence for Pre- and Postmineralization Diatremes in the Tujuh Bukit District, Southeast Java, Indonesia. Econ. Geol. 113, 163–192.

Hedenquist, J.W., Arribas, A., Reynolds, T.J., 1998. Evolution of an intrusion-centered hydrothermal system; Far Southeast-Lepanto porphyry and epithermal Cu-Au deposits, Philippines. Econ. Geol. 93, 373–404.

Heinrich, C.A., Driesner, T., Stefánsson, A., Seward, T.M., 2004. Magmatic vapor contraction and the transport of gold from the porphyry environment to epithermal ore deposits. Geology 32, 761–764.

Herman, F., Seward, D., Valla, P.G., Carter, A., Kohn, B., Willett, S.D., Ehlers, T.A., 2013. Worldwide acceleration of mountain erosion under a cooling climate. Nature 504, 423–426.

Hollister, V., 1977. Kinematics and regional tectonic interpretation of the east-trending fold belt of Peru. Geol. Soc. Am. Bull. 88, 1749–1755.

Jansen, N.H., Gemmell, J.B., Chang, Z., Cooke, D.R., Jourdan, F., Creaser, R.A., Hollings, P., 2017. Geology and genesis of the Cerro la Mina porphyry-high sulfidation Au (Cu-Mo) prospect, Mexico. Econ. Geol. 112, 799–827.

Kesler, S.E., Wilkinson, B.H., 2006. The role of exhumation in the temporal distribution of ore deposits. Econ. Geol. 101, 919–922.

Longo, A.A., 2005. Evolution of volcanism and hydrothermal activity in the Yanacocha mining district, northern Perú. Oregon State University, Corvallis, USA. Ph. D thesis.

Longo, A.A., Dilles, J.H., Grunder, A.L., Duncan, R., 2010. Evolution of calc-alkaline volcanism and associated hydrothermal gold deposits at Yanacocha, Peru. Econ. Geol. 105, 1191–1241.

Lonsdale, P., 2005. Creation of the Cocos and Nazca plates by fission of the Farallon plate. Tectonophysics 404, 237–264.

Lovera, O.M., Grove, M., Mark Harrison, T., Mahon, K.I., 1997. Systematic analysis of K-feldspar 40Ar/39Ar step heating results: I. Significance of activation energy determinations. Geochim. Cosmochim. Acta 61, 3171–3192.

Marinov, D., 2011. Re-Os Molybdenite Geochronology from Michiquillay and Galeno Porphyry Copper Deposits, Cajamarca, Perú. 11th Biennial Meeting, SGA 2011 Antofagasta, Chile.

Masterman, G.J., Cooke, D.R., Berry, R.F., Walshe, J.L., Lee, A.W., Clark, A.H., 2005. Fluid chemistry, structural setting, and emplacement history of the Rosario Cu-Mo porphyry and Cu-Ag-Au epithermal veins, Collahuasi district, northern Chile. Econ. Geol. 100, 835–862.

Maydagán, L., Zattin, M., Mpodozis, C., Selby, D., Franchini, M., Dimieri, L., 2020. Apatite (U–Th)/He thermochronology and Re–Os ages in the Altar region, Central Andes (31°30′S), Main Cordillera of San Juan, Argentina: implications of rapid exhumation in the porphyry Cu (Au) metal endowment and regional tectonics. Miner. Deposita 55, 1365–1384.

McDougall, I., Harrison, T.M., 1999. Geochronology and Thermochronology by the 40Ar/39Ar Method. Oxford University Press, New York.

McInnes, B.I.A., Evans, N.J., Fu, F.Q., Garwin, S., Belousova, E., Griffin, W.L., Bertens, A., Sukarna, D., Permanadewi, S., Andrew, R.L., Deckart, K., 2005. Thermal History Analysis of Selected Chilean, Indonesian and Iranian Porphyry Cu-Mo-Au Deposits. Super Porphyry Copper & Gold Deposits: A Global Perspective, PGC Publishing, Adelaide, pp. 27–42.

McLaughlin, D.H., 1924. Geology and physiography of the Peruvian Cordillera, departments of Junin and Lima. Geol. Soc. Am. Bull. 35, 591–690.

Mégard, F., 1984. The Andean orogenic period and its major structures in central and northern Peru. J. Geol. Soc. London 141, 893–900.

Mégard, F., Noble, D.C., McKee, E.H., Cuénod, Y., 1985. Tectonic significance of silicic dikes contemporaneous with latest Miocene Quechua 3 tectonism in the Rimac valley, western Cordillera of central Peru. J. Geol. 93, 373–376.

Montgomery, A.T., 2012. Metallogenetic controls on Miocene high sulphidation epithermal gold mineralization, Alto Chicama district, La Libertad, Northern Peru. Queen's University, Kingston, Canada. Ph. D thesis.

Muntean, J.L., Einaudi, M.T., 2001. Porphyry-epithermal transition: Maricunga belt, northern Chile. Econ. Geol. 96, 743–772.

Murakami, H., Seo, J.H., Heinrich, C.A., 2010. The relation between Cu/Au ratio and formation depth of porphyry-style Cu–Au±Mo deposits. Miner. Deposita 45, 11–21.

Navarro, P.A., Rivera, M.A., Monge, R.W., 2010. Geología y metalogenia del Grupo Calipuy (Volcanismo Cenozoico) segmento Santiago de Chuco, norte del Perú. Instituto Geológico Minero y Metalúrgico. Lima, Perú: Boletín Serie D: Estudios Regionales no. 28.

Noble, D.C., McKee, E.H., 1999. The Miocene Metallogenic Belt of Central and Northern Perú. Geology and Ore Deposits of the Central Andes. Soc. Econom. Geol. 155–193.

Noble, D.C., McKEE, E.H., Mourier, T., Mégard, F., 1990. Cenozoic stratigraphy, magmatic activity, compressive deformation, and uplift in northern Peru. Geol. Soc. Am. Bull. 102, 1105–1113.

Noble, D.C., Vidal, C.E., Perelló, J., Rodríguez, O., 2004. Space-Time Relationships of Some Porphyry Cu-Au, Epithermal Au, and Other Magmatic-Related Mineral Deposits in Northern Peru. New Discoveries, Concepts, and Updates. Society of Economic Geologists, Andean Metallogeny, pp. 313–318.

Pan, J.-Y., Ni, P., Chi, Z., Wang, W.-B., Zeng, W.-C., Xue, K., 2019. Alunite $^{40}Ar/^{39}Ar$ and Zircon U-Pb Constraints on the Magmatic-Hydrothermal History of the Zijinshan High-Sulfidation Epithermal Cu-Au Deposit and the Adjacent Luoboling Porphyry Cu-Mo Deposit, South China: Implications for Their Genetic Association. Econ. Geol. 114, 667–695.

Pardo-Casas, F., Molnar, P., 1987. Relative motion of the Nazca (Farallon) and South American plates since Late Cretaceous time. Tectonics 6, 233–248.

Prudhomme, A., Baby, P., Robert, A., Brichau, S., Cuipa, E., Eude, A., Calderon, Y., O'Sullivan, P., 2019. Western thrusting and uplift in northern Central Andes (western Peruvian margin). Andean Tectonics 299–331.

Rainbow, A., Clark, A.H., Kyser, T.K., Gaboury, F., Hodgson, C.J., 2005. The Pierina epithermal Au–Ag deposit, Ancash, Peru: paragenetic relationships, alunite textures, and stable-isotope geochemistry. Chem. Geol. 215, 235–252.

Ramos, V.A., Folguera, A., 2009. Andean flat-slab subduction through time. Geol. Soc. Lond. Spec. Publ. 327, 31–54.

Richards, J.P., 2011. Magmatic to hydrothermal metal fluxes in convergent and collided margins. Ore Geol. Rev. 40, 1–26.

Rinne, M.L., Cooke, D.R., Harris, A.C., Finn, D.J., Allen, C.M., Heizler, M.T., Creaser, R. A., 2018. Geology and Geochronology of the Golpu Porphyry and Wafi Epithermal Deposit, Morobe Province, Papua New Guinea. Economic Geology 113, 271–294.

Rosenbaum, G., Giles, D., Saxon, M., Betts, P.G., Weinberg, R.F., Duboz, C., 2005. Subduction of the Nazca Ridge and the Inca Plateau: Insights into the formation of ore deposits in Peru. Earth Planet. Sci. Lett. 239, 18–32.

Rottier, B., Kouzmanov, K., Casanova, V., Wälle, M., Fontboté, L., 2018. Cyclic Dilution of Magmatic Metal-Rich Hypersaline Fluids by Magmatic Low-Salinity Fluid: A Major Process Generating the Giant Epithermal Polymetallic Deposit of Cerro de Pasco, Peru. Econ. Geol. 113, 825–856.

Rousse, S., Gilder, S., Farber, D., McNulty, B., Patriat, P., Torres, V., Sempere, T., 2003. Paleomagnetic tracking of mountain building in the Peruvian Andes since 10 Ma. Tectonics 22.

Santos, A., 2020. Lithocap on porphyry shoulder: Geology and lifespan of the La Arena-Calaorco porphyry and epithermal deposits, Huamachuco-Cajabamba Belt, Northern Peru. China University of Geosciences, Wuhan, China. M.Sc thesis.
Scherrenberg, A.F., Kohn, B.P., Holcombe, R.J., Rosenbaum, G., 2016. Thermotectonic history of the Maranon Fold-Thrust Belt, Peru: Insights into mineralisation in an evolving orogen. Tectonophysics 667, 16–36.
Sébrier, M., Soler, P., 1991. Tectonics and magmatism in the Peruvian Andes from late Oligocene time to the Present. In: Harmon, R.S., Rapela, C.W. (Eds.), Andean Magmatism and Its Tectonic Setting. Geological Society of America, pp. 259-278.
Sillitoe, R.H., 1972. A plate tectonic model for the origin of porphyry copper deposits. Econ. Geol. 67, 184–197.
Sillitoe, R.H., 1973. The tops and bottoms of porphyry copper deposits. Econ. Geol. 68, 799–815.
Sillitoe, R.H., 1994. Erosion and collapse of volcanoes: Causes of telescoping in intrusion-centered ore deposits. Geology 22, 945–948.
Sillitoe, R.H., 2010. Porphyry copper systems. Econ. Geol. 105, 3–41.
Sillitoe, R.H., Perelló, J., 2005. Andean copper province: Tectonomagmatic settings, deposit types, metallogeny, exploration, and discovery. Economic Geology 100th Anniversary Volume, 845-890.
Sillitoe, R.H., Mortensen, J.K., 2010. Longevity of porphyry copper formation at Quellaveco, Peru. Econ. Geol. 105, 1157–1162.
Sillitoe, R.H., 2000. Gold-Rich Porphyry Deposits: Descriptive and Genetic Models and Their Role in Exploration and Discovery. In: Hagemann, S.G., Brown, P.E. (Eds.), Gold in 2000. Society of Economic Geologists, pp. 315-345.
Snee, L.W., Sutter, J.F., Kelly, W.C., 1988. Thermochronology of economic mineral deposits; dating the stages of mineralization at Panasqueira, Portugal, by high-precision 40Ar/39Ar age spectrum techniques on muscovite. Econ. Geol. 83, 335–354.
Somoza, R., 1998. Updated Nazca (Farallon)—South America relative motions during the last 40 My: implications for mountain building in the central Andean region. J. S. Am. Earth Sci. 11, 211–215.
Steinmann, G., 1929. Geologie von Perú. Carl Winterss Universitats Buch Handlung, Heidelberg, p. 448.
Suzuki, K., Shimizu, H., Masuda, A., 1996. Re-Os dating of molybdenites from ore deposits in Japan: Implication for the closure temperature of the Re-Os system for molybdenite and the cooling history of molybdenum ore deposits. Geochim. Cosmochim. Acta 60, 3151–3159.
Tosdal, R. M., Richards, J. P., 2001. Magmatic and Structural Controls on the Development of Porphyry Cu ± Mo ± Au Deposits. In: Richards, J.P., Tosdal, R.M. (Eds.), Structural Controls on Ore Genesis. Society of Economic Geologists, pp. 157-181.
USGS (2022) Mineral commodity summaries 2021. https://pubs.er.usgs.gov/publication/mcs2022.
von Quadt, A., Erni, M., Martinek, K., Moll, M., Peytcheva, I., Heinrich, C.A., 2011. Zircon crystallization and the lifetimes of ore-forming magmatic-hydrothermal systems. Geology 39, 731–734.
Weis, P., Driesner, T., Heinrich, C.A., 2012. Porphyry-Copper Ore Shells Form at Stable Pressure-Temperature Fronts Within Dynamic Fluid Plumes. Science 338, 1613.
Wolf, R.A., Farley, K.A., Silver, L.T., 1996. Helium diffusion and low-temperature thermochronometry of apatite. Geochim. Cosmochim. Acta 60, 4231–4240.
Yanites, B.J., Kesler, S.E., 2015. A climate signal in exhumation patterns revealed by porphyry copper deposits. Nat. Geosci. 8, 462–465.
Yin, J., Chen, W., Thomson, S.N., Sun, M., Wang, Y., Xiao, W., Yuan, C., Sun, J., Long, X., 2019. Fission track thermochronology of the Tuwu-Yandong porphyry Cu deposits, NW China: Constraints on preservation and exhumation. Ore Geol. Rev. 113, 103104.